RSC Advances

ROYAL SOCIETY OF CHEMISTRY

www.rsc.org/advances

The larger area graphene formation from the small GO sheet in presence of basic divalent sulfide species and its usage in biomass conversion

Xuyan Wang[1], Kunmei Su[1], Zhenhuan Li*[2], Bowen Cheng*[2]

[1]State Key Laboratory of Separation Membranes and Membrane Processes, School of environment Science and Chemisty Engineering, Tianjin Polytechnic University, Tianjin, China

[2]School of Materials Science and Engineering, Tianjin Polytechnic University, 300387, Tianjin, China

Abstract: The basic divalent sulfide exhibits a unique chemical activity both in its ability to react with organic matter and as a redox reagent. Herein, graphene oxide (GO) was modified by basic divalent sulfide species, and the modified materials were characterized by FT-IR spectra, XRD, UV-Vis, SEM, HRTEM, XPS, TG-MS analysis, Raman spectroscopy and electrical conductivity measurement. The characterized results indicated that basic divalent sulfide could well remove the abundant oxygen-containing groups on the basal-plane of GO, in which the π-conjugated structure was largely restored. However, the basic divalent sulfide species can also react with marginal oxygen-containing groups and be doped into GO to form large-area π-conjugated structure to result in the high electrical conductivity of sulfur modified GO (SGO). TG-MS analysis showed that the basic divalent sulfide in SGO can be well removed under heating conditions, which provides a new method to realize the larger area graphene sheet preparations from GO of smaller average size. In addition, the prepared SGO without annealing displayed a better performance in fructose, glucose, cellobiose and cellulose conversion to 5-hydroxymethylfurfural (HMF) because it remained some acidic marginal oxygen-containing groups and basic divalent sulfide species.

Keywords: Graphene oxide, the larger area graphene formation, S incorporation, Basic divalent sulfide, 5-hydroxymethylfurfural

Introduction

Graphene, a single layer of sp^2-bonded carbon atoms arranged in a honeycomb structure,[1] has attracted much attention for its unique electronic properties, excellent mechanical properties, and superior thermal properties.[2] To date, the approaches to prepare graphene contained mechanical exfoliation of bulk graphite,[3] epitaxial growth,[4] chemical vapor deposition[5] and chemical reduction of GO [6] et al. Among them, the chemical reduction of GO is the most efficient method for low-cost and large-scale production of graphene. In the chemical reduction process, GO, known as a material rich in oxygen containing groups such as hydroxyl, carbonyl and epoxy group, was produced by the well-known Hummers method,[7] and the reduced graphene oxide was obtained by the chemical reduction of GO using a suitable reducing agent. As a sort of efficient reducing agents, hydrazine, [8] $NaBH_4$,[9] ascorbic acid,[10] HI,[11] $NaHSO_3$, [12] $Na_2S_2O_4$ [13, 14] et al had been used to reduce GO, and among them hydrazine and $NaBH_4$ were effective in removing oxygen of GO. However, when N_2H_4 was used as reducing agent, N was doped in the as-prepared graphene[9]. Although $NaBH_4$ showed excellent ability in GO reduction, the hydrolysis property made it difficult to get a stable $NaBH_4$ aqueous solution, resulting in low efficiency in reduction[15].

Since the bond energy of C-S is weaker than that of C-N, using sulfur-containing compounds as the reducing agent may allow GO deoxygenation more easily.[16] Therefore sulfur-containing compounds, such as $NaHSO_3$, $Na_2S_2O_3$ and SO_2,[17] have been used as reducing agents to reduce GO. It is well-known that the basic divalent sulfide species are efficient reducing agents and can react with functionalized organic compounds to form organic sulfur compound. Although the reductive reaction induced by sulfur-containing compounds

was expected to have little influence on the marginal carboxyl and hydroxyl groups owing to the high-energy barrier,[16] the basic divalent sulfide species could open up epoxy groups to form hydroxyls.[18] These characteristics might facilitate a complex network of chemical reactions during GO modification by basic divalent sulfide, including the reductive deoxygenation reaction on the basal planes of pristine GO and the sulfur incorporation by the nucleophilic reaction between basic divalent sulfide species and peripheral oxygen containing groups (carbonyl and hydroxyl) of GO.

In this paper, GO was modified by basic divalent sulfide species, and it was found that the basic divalent sulfide could remove the abundant hydroxyl and epoxide functionalities on basal-plane of GO, and sulfur can also be incorporated into SGO to form the large-area graphene sheets through GO sheet connection. According to the anthraquinone reduction by basic divalent sulfide species,[19] the mechanism of GO deoxygenation and sulfur incorporation were provided. In addition, SGO was used to catalyze biomass conversion into HMF, which provided some more information about sulfur incorporation.

2. Experiment section

2.1. Material preparation

GO was prepared from natural graphite powder (Purchased from Tianjin Kermel Chemical Reagent Co., Ltd) by the Hummers method.[7] In a typical GO modification procedure, 1g GO and 500 mL water were loaded in a 1000 mL round bottom flask, and this homogeneous mixture was sonicated using a KQ3200 ultrasonic bath cleaner (150 W) for 4h. After that 15 g K_2S or Na_2S (94.7%, Yili Company) and 2 g NaOH (analytical grade, Sinopharm Chemical Reagent Co.,Ltd) were added gradually (1 g/min) to above suspension

at 98 °C. The color of mixture turned from pale yellow (or brown) to black after 24 h, and SGO precipitation appeared. SGO was obtained by filtration, and it was washed using deionized water until the PH of eluate reached 7. SGO was dried at 60 °C for 24 h under the vacuum condition.

GO modification by N_2H_4 was also carried out under the similar conditions (N_2H_4 Tianjin Beifang Tianyi Chemical Reagent Company, 80%), namely 3 mL N_2H_4 (80%, Tianjin Beifang Tianyi Chemical Reagent Company) and 2 g NaOH (analytical grade, Sinopharm Chemical Reagent Co., Ltd) were added to the above GO suspension. The mixture was heated to 98 °C with the assistance of vigorous stirring (300 r/min). After 24 h, the color of the mixture turned from pale yellow (or brown) to black, and the RGO precipitation appeared. After filtration, the precipitation was washed using deionized water until the PH of the eluate reached 7. The product was dried at 60 °C for 24 h under the vacuum condition. The undoped TRGO was obtained by thermal reduction method at 800 ^{o}C in presence of Ar atmosphere.

2.2. Biomass conversion process

The catalytic experiments were performed in a 20 ml flask. In a typical experiment, 0.9 g glucose and 0.03 g catalyst were added into 5 ml [EMIM]Br. After reaction system had been purged with nitrogen, the reaction mixture was heated in an oil-bath at 140 ^{o}C for 4 h. After the desired reaction time elapsed, reaction mixture was cooled to room temperature immediately.

2.3. Characterization

HRTEM images were obtained from a JEM-2100 transmission electron microscope (JEOL, Japan) and SEM images from a Hitachi 4800S electron microscope (Japan). Raman spectra were obtained using a 514.5 nm argon ion laser with a high resolution via Raman

Microscope (RENISHAW, UK). UV-Vis absorption spectra were recorded on a TU-1901 UV-Vis spectrophotometer (ThermoFisher). FT-IR spectra of the samples were recorded on a TENSOR 37 (BRUKER Corporation, Germany) using KBr-disk method. Thermal properties were characterized by TG (STA409 PC thermogravimetry, NETZSCH, Germany) connected to a Mass Spectrometry analyzer. This measurement was carried out at a heating rate of 5 °C/min in N_2 atmosphere in the temperature range from 25 °C to 800 °C. The crystal structure was characterized by X-ray diffraction (XRD, Elmer PHI-5600) with Mg Kα radiation. X-ray photoelectron spectroscopy (XPS, ThermoFisher K-alpha) characterized the C/O ratio and the change of functional groups. XPS peak deconvolution was carried out using XPS peak 4.1 software in which a Shirley background was assumed. Electrical conductivity was measured by a four-probe method and the corresponding volume conductivity (σ, S/cm) was calculated using the formula: $\sigma = 1/\rho$, where ρ (unit: Ω·cm) refers to the electrical resistivity. N_2 adsorption-desorption isotherms were obtained on a Autosorb-iQ analyzer at -196 ^{o}C. Prior to the adsorption-desorption measurements, all samples were degassed at 150 ^{o}C overnight under a vacuum condition.

HMF yield was analyzed by the high performance liquid chromatograph (a 996 photodiode array detector and Waters1525 equipped with UV). HMF yield was quantified with a Kromasil C18 (250×4.6mm, 5um) reverse phase column, using a mobile phase CH_3OH-H_2O (80:20) at a flow rate of 1.0mL/min, and HMF yield was based on hexose loading.

$$5\text{-HMF yield}\,(\text{mol}\%) = \frac{moles\ of\ HMF}{moles\ of\ hexose} \times 100\%$$

3. Results and discussion

3.1 Graphene characterization

The modification of GO in the presence of basic divalent sulfide can be easily observed by the color change of mixture, from brown to black. After modification, the black SGO precipitated out from the solution. Fig 1a showed the FT-IR spectra of GO and SGO. The characteristic peaks of GO contains carbonyl C=O (1735 cm^{-1}), hydroxyl O-H (1380 cm^{-1}), carboxy C-O (1230 cm^{-1}) and epoxy C-O (1065 cm^{-1}).[20] The broad peak at 3500 cm^{-1} was assigned to the vibrations of hydroxyl groups. After GO modification by N_2H_4 (NGO), two new peaks appeared at 3418 cm^{-1} and 3126 cm^{-1}, indicating the doping of N. As for the C-H stretching vibration at 2800-3000 cm^{-1}, those peaks of SGO were much weaker than that of NGO, which confirmed the efficient restoration of the conjugated structure in presence of basic divalent sulfide species. In addition, it could be observed that a weak visible absorption at 410 nm for SGO, which suggested sulfide incorporation.

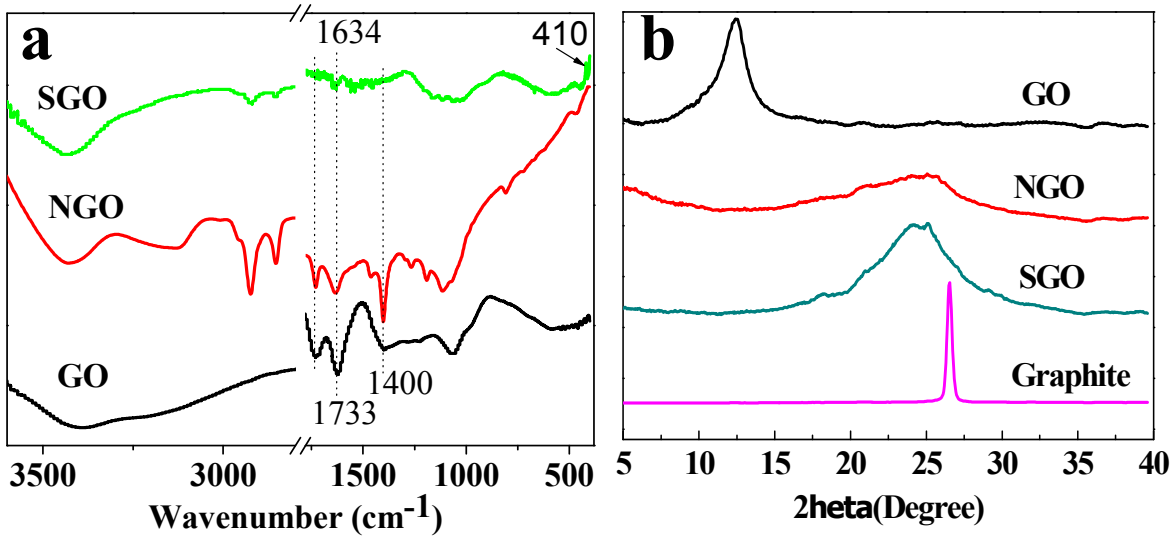

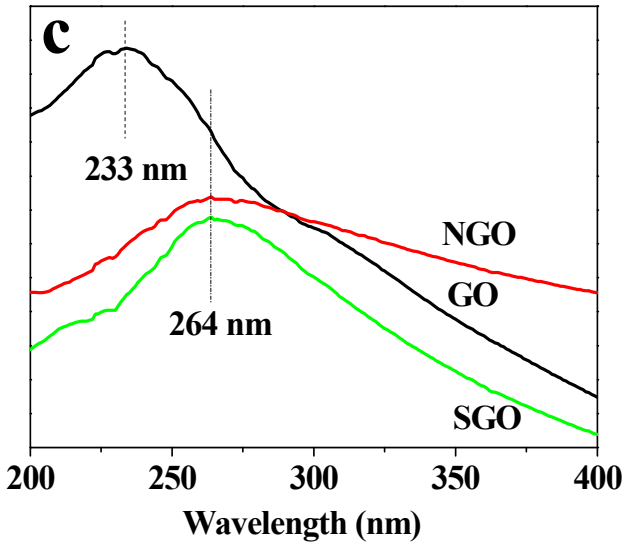

Fig. 1 Characterization of GO, SGO and NGO: (a) FTIR spectra; (b) XRD patterns of graphite, GO, SGO and NGO. (c) UV-Vis absorption spectra.

Fig.1 b showed the XRD patterns of GO, graphite, SGO and NGO. The diffraction peak at 2θ = 12.5° confirmed the relatively complete exfoliation of graphite.[21] The interlayer distance obtained from the (002) peak of graphite was 3.46 Å (2θ = 25.70°), which was expanded to 7.10 Å (2θ = 12.45°) after oxidation by the Hummers method, indicating the formation of oxygen-containing groups such as hydroxyl, epoxy and carboxyl groups.[22] After GO modification by N_2H_4 and basic divalent sulfide, the intensive peak of GO at 2θ = 12.45° disappeared, and the new broadened peaks at 2θ = 24.3° and 2θ = 25.1° appeared. The interlayer distance of NGO and SGO returned back to 3.69 and 3.55 Å, respectively, which implied the removal of the most oxygen functional groups and the disorder agglomeration of planar sheet by π-π stacking interactions.

Fig. 1c showed a maximum UV-Vis absorption peak at 233 nm in GO, which was mainly due to the π-π^* transition of aromatic C-C bonds in GO.[23] After GO modification, the

absorption peak shifted to the red region, reaching a value of 264 nm. Those results indicated that the extended π-π conjugated structure of GO had been significantly destroyed during oxidization. However, as the deoxygenation took place, the extensive conjugated sp^2-carbon network has been rebuilt in the modifying process.[24] By the comparison of NGO with SGO, it was found that NGO showed obvious visible light absorption extending up to 400 nm, while almost no visible absorption can be seen at 400 nm for SGO, which suggested sulfide was incorporated into SGO.

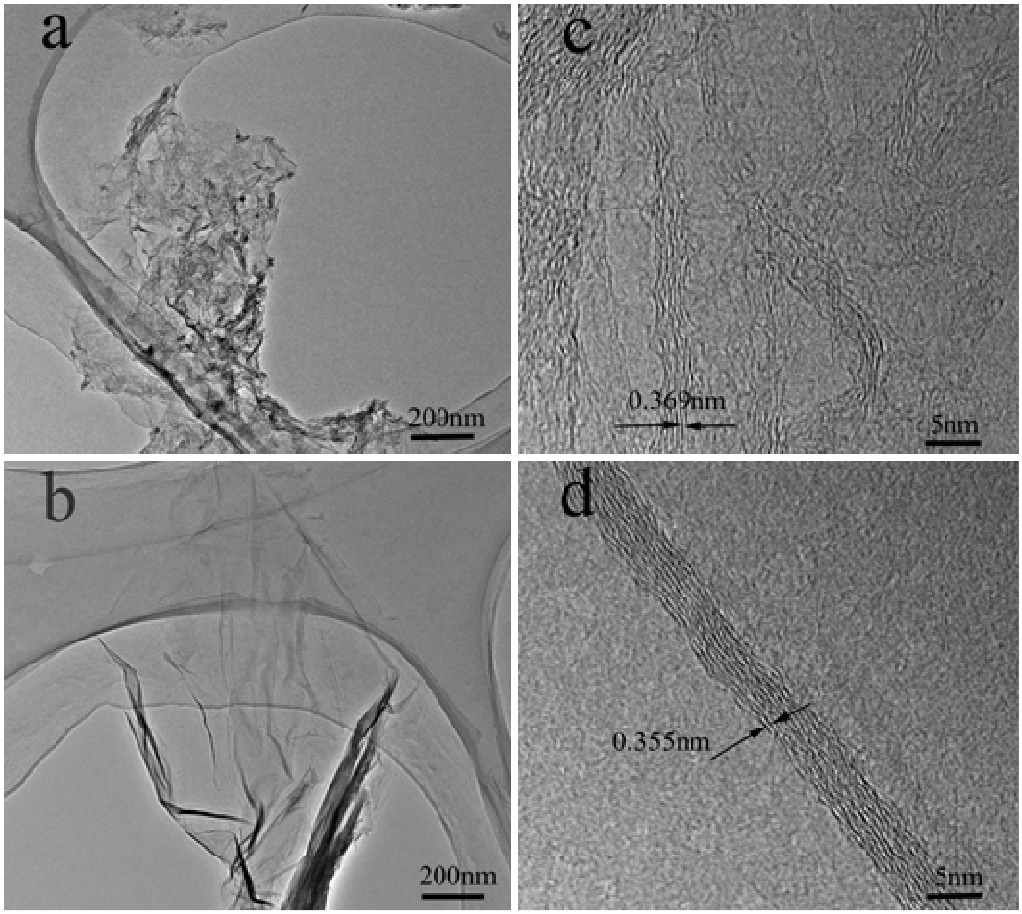

Fig. 2. HRTEM image of NGO (a and c) and SGO (b and d).

Fig. 2 showed the HRTEM images of NGO and SGO. HRTEM images revealed the layered structure of the reduced material. As shown in Fig 2a, GO modification by N_2H_4 was observed with more wrinkled structures, and these small sheets were randomly aggregated

and closely associated with each other in a low magnification. The corrugations are attributed to the disruption of the planar sp^2 carbon sheets and the existence of some residual sp^3-hybridized carbon on graphene sheets. As shown in Fig 2b, SGO showed a transparent, bulk planar sheet and wrinkled paper-like structure, which indicated that SGO exhibited a better and larger sheet area than NGO. Congruent with XRD results, the edge-on HRTEM image of NGO (Fig 2c) showed an inter-graphene spacing of 0.369 nm, while the inter-graphene spacing of SGO declined to 0.355 nm. Further more, the HRTEM images of NGO from an edge-on view also showed graphene sheets arranged in a disordered structure. However, there existed the ordered stacking of larger sheet in SGO, which indicated the well restored conjugated structure of SGO and the sulfur incorporation among GO sheets into the larger area graphene. To prove the existed connection between small GO sheets after the sulfide reduction, TEM images of SGO, GO and NGO with low magnification were provided in Fig. 3, which further proved that the size of SGO is apparently larger than that of GO and NGO. From those low magnification TEM images, we can conclude that some small pieces of GO were connected into larger pieces of SGO during GO reduction by basic divalent sulfide species.

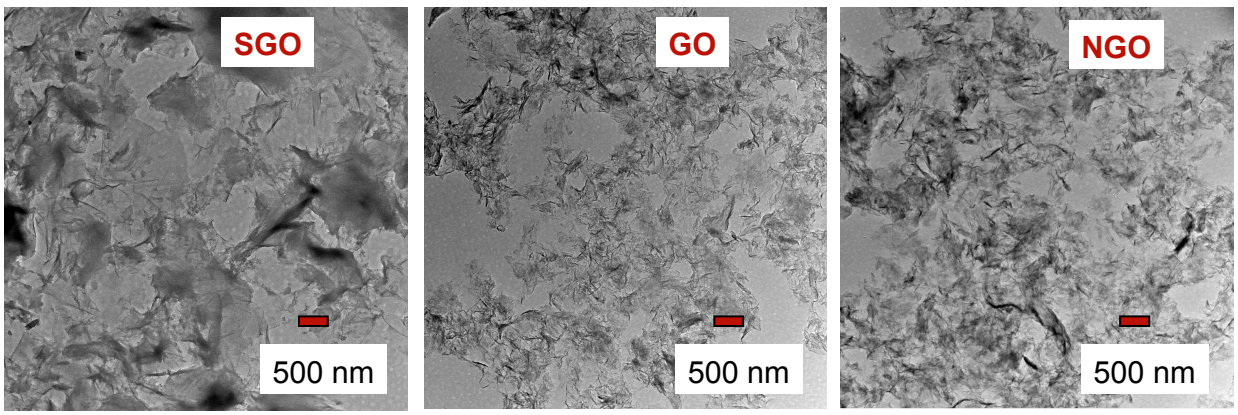

Fig. 3. the low magnification TEM image of SGO, GO and NGO

GO, NGO and SGO were characterized by XPS, and the characterized results were shown in Fig 4. C1s XPS spectra of GO were deconvoluted into four peaks according to the carbon atoms in different chemical states. GO contains the non-oxygenated C (C-C/C=C, 284.8 eV), hydroxyl or epoxy C (C-O 285.8 eV), carbonyl C (C=O, 287.6 eV) and the carboxyl C (-O-C=O, 288.8 eV).[25, 26] After the chemical modification by basic divalent sulfide, the oxygen species of C-O (hydroxyl and epoxyl), C=O (carbonyl) and O=C-O (carboxyl) reduced significantly, which indicated an efficient deoxidization. The remaining specie was sp^2 C=C, while SP^3 C-C (285.1eV) and C=O species were completely removed. In addition, a trace of the marginal O=C-O (288.8eV) and C-OH (285.8 eV) existed after modification, and some C-S (285.3 eV) also exited in SGO. As shown in Fig 3d, when GO was modified by N_2H_4, a new intensive SP^3 C-C (285.1eV) peak existed, which conformed the existence of saturated C-H in NGO. Be similar with SGO, some O=C-O also existed after N_2H_4 reduction, but a new peak at 286.3 eV appeared due to C=N formation. Those results were consistent with FT-IR characterization. After GO modification by basic divalent sulfide, C/O ratio increased from 1.95 to 4.98 which was comparable to GO reduced by $NaBH_4$,[27] indicating an efficient deoxidization. N1s XPS spectra and S2p XPS spectra of GO, NGO and SGO were listed in Fig.4e and Fig.4f, and those characterized results also conformed the formation of C-N bonds in NGO (N1s peak appearance at 400.0 eV) and the existence of C-S bonds in SGO (S2p peak at 164.4 eV). Because S was incorporated at low temperature (98 ^oC), some C-S peaks around 285.3 eV exited and the S peak at 164.4 eV appeared, which is attributed to the S existence inside the lattice structure of the graphene and it is covalently bonded to the graphene in the form of thiophenic, disulfide and thioether species.[28] In

addition, a weak S2p peak at 169.1 eV was also detected in GO and SGO, which was attributed to a trace of SO_3H existence. Those results also indicated GO can be sulfonated during the exfoliation of graphite, but sulfonic acid group can be eliminated by N_2H_4 reduction

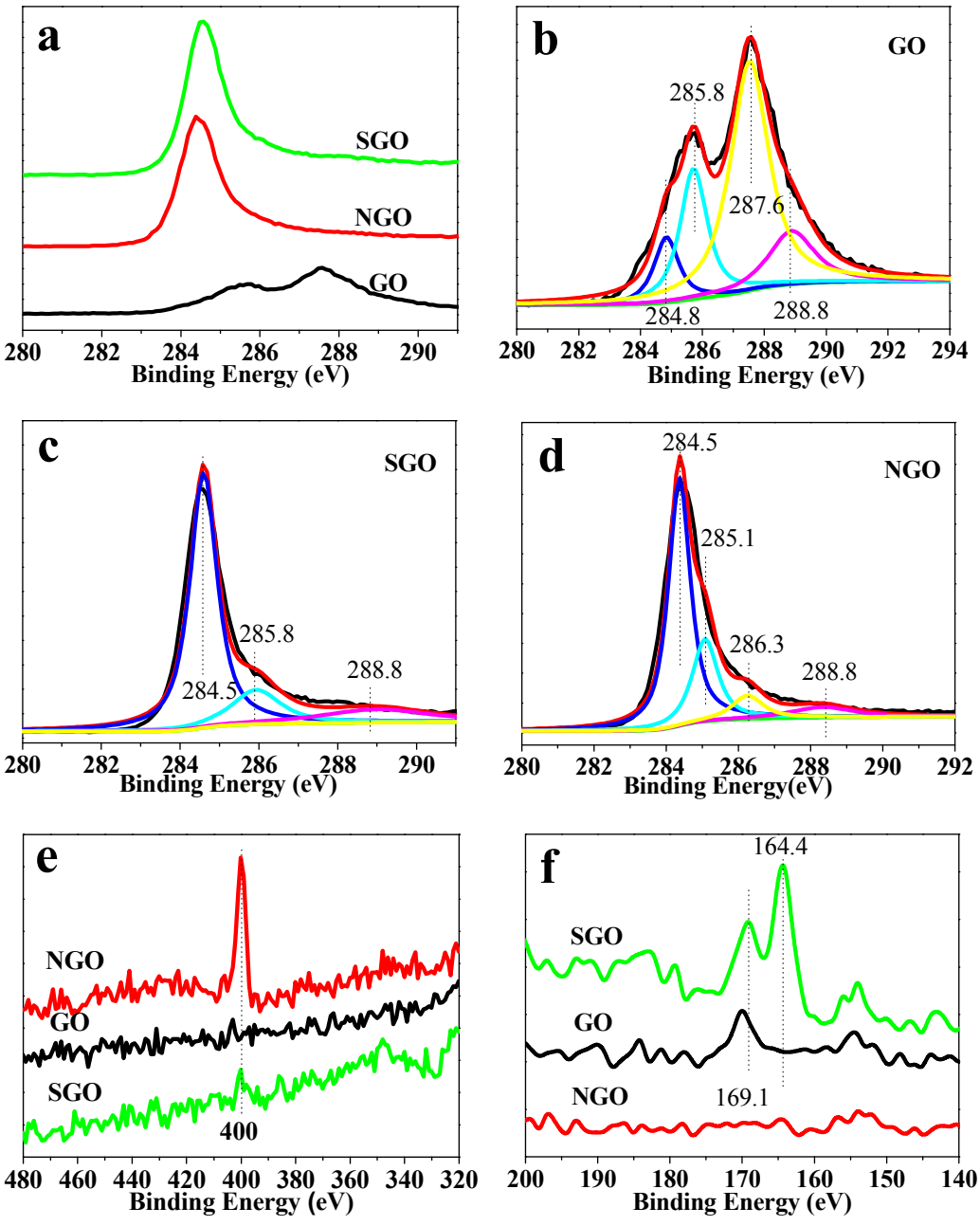

Fig 4. (a) is the C1s spectra of GO, SGO and NGO; (b-d) are the deconvoluted C1s spectra of the ones of each samples. (e) N1s X-ray photoelectron spectra of GO, NGO and SGO; (f) S2p

X-ray photoelectron spectra of GO, NGO and SGO.

As shown in Fig. 5, Fig.5a displayed the TGA curves of GO, NGO and SGO, and Fig.5 b~d showed the mass intensity profiles of different thermal decomposition product from GO, BGO and SGO. TGA curves of GO, NGO and SGO displayed a small weight loss around 100 °C, mainly due to the adsorbed water. The major mass loss of GO took place at around 200 °C, and the mass loss was ascribed to the gaseous escape of H_2O and CO_2, indicating the decomposition of oxygen-containing groups that were thermally unstable. The minor mass loss of GO took place at 500-800 °C, which was mainly attributed to H_2O escape, while only a trace of CO_2 gas was detected at around 600 °C. In contrast with GO, NGO and SGO exhibited a less weight loss in the temperature range from room temperature to 800 °C, and the mass loss at around 200 °C was small, indicating the efficient removal of oxygen functional groups after modification. As for NGO, the mass loss was attributed to the removal of absorbed H_2O, produce of NH_3 from the decomposition of C-N species and escape of CO_2 from residual oxygen functional groups (see Fig 3c). The release of CO_2 inevitably left behind vacancies and topological defects on the graphene sheets, and single carbon vacancies could coalesce into double vacancy and result in topological defects lined up along the wrinkle. It was interesting to note here that the thermal stability of NGO was a little better than that of SGO, which was mainly attributed to S elimination from SGO (see Fig 3d). Oxygen, nitrogen and carbon were released as relatively non-active low-molecular-weight compounds (e.g. CO_2, H_2O, NH_3), but sulfur often was released as highly active species, such as H_2S, S element and polysulfide ions. Herein, S element was detected as the main escaping specie during SGO thermal cleavage

process at 167, 267, 493, 756 and 900 °C.

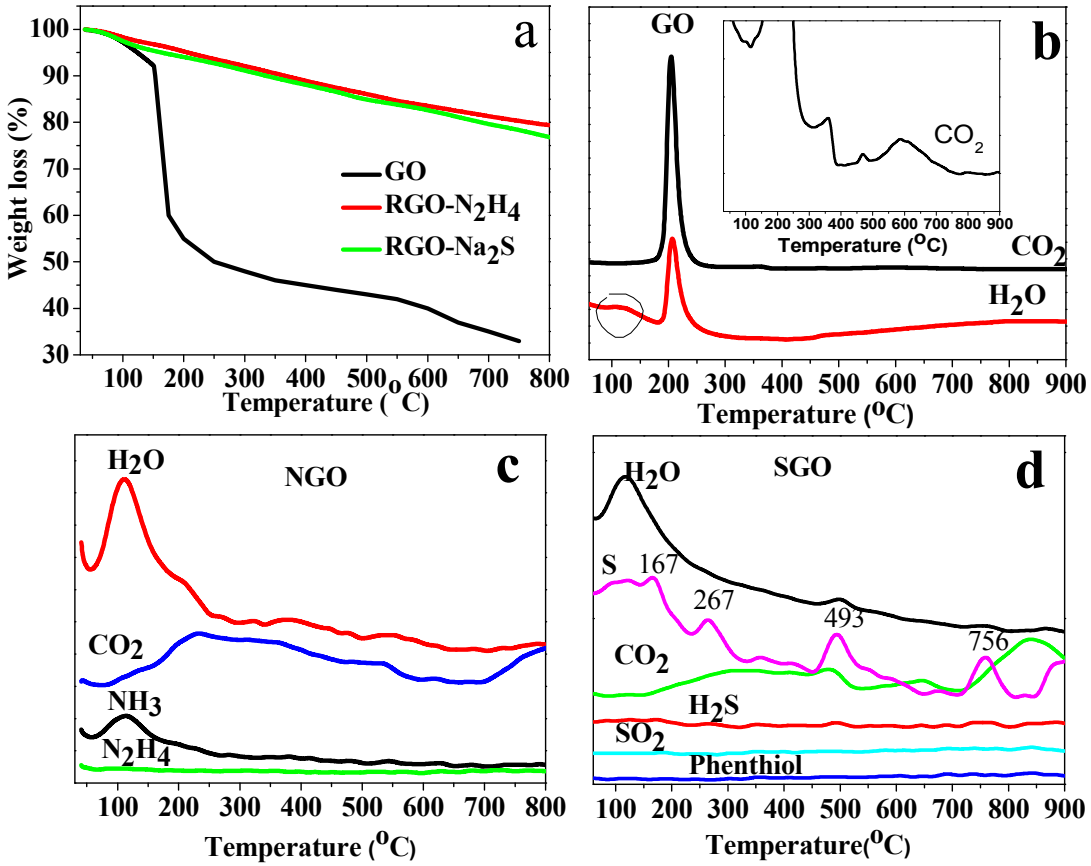

Fig 5. TG and TG-MS curves of GO, NGO and SGO: (a) TG curves of GO, NGO and SGO; (b) Mass intensity profiles of H_2O and CO_2 from GO TG-MS curves; (c) Mass intensity profiles of H_2O, CO_2, NH_3 and N_2H_4 from NGO TG-MS curves; (d) Mass intensity profiles of H_2O, CO_2, S, SO_2 and phenthiol from SGO TG-MS curves. The inset of Fig 4b is the Mass intensity profiles of CO_2, which can be viewed as the amplification of the black line in Fig 4b. We use the inset to confirm the trace of CO_2 escape around 600 °C.

The significant changes of GO structure during the chemical modification processing were recorded in the Raman spectrum in Fig 6. The spectrum of GO displayed two peaks, that was D band at around 1364 cm^{-1} and G band at around 1592 cm^{-1}. The I_D/I_G ratio was often used to

estimate the defect of the sample and the in-plane crystallite sizes in disordered carbon materials.[29, 30] I_D/I_G ratio of GO was 0.76, which increased to 0.90 of SGO and 0.96 of NGO, indicating the modification in size of the in-plane sp^2 domains. As for SGO and NGO, the G band moved to 1584 cm^{-1}, which was close to the value of the pristine graphite, confirming the reduction of GO during the chemical modification. Those changes suggested more sp^2 domain formation and the decrease in the average size of the sp^2 domains upon modification of the exfoliated GO.[6,31] Most importantly, the I_D/I_G ratio of GO was slightly lower than that of modified GO, which was possibly related to the ordered stacking of GO layers by the numerous hydrogen bonds. The above conclusion was consistent with the earlier reports that the reduction of GO increased the number of aromatic domains of smaller average size in graphene and led to an increase of the I_D/I_G ratio.[6] However, I_D/I_G ratio of SGO was slightly lower than that of NGO, indicating the aromatic domains of smaller average size in NGO while the large-area π-conjugated structure formation through GO sheets connection by basic divalent sulfide species.

Besides the D and G bands, both GO and modified GO contains 2D peak and D+G peak at 2710 cm^{-1} and 2926 cm^{-1} respectively. The 2D band is a characteristic band for defect-free graphitic structures, whereas the D+G band is induced by structural disorder.[32] As for GO, NGO and SGO, the I_{2D}/I_{D+G} ratios were 0.78, 0.79 and 0.91, respectively, strongly suggesting the restoration of sp^2 carbon in modified GO.[33] The I_{2D}/I_{D+G} ratio of SGO was higher than that of NGO, indicating the less defection formation in SGO.

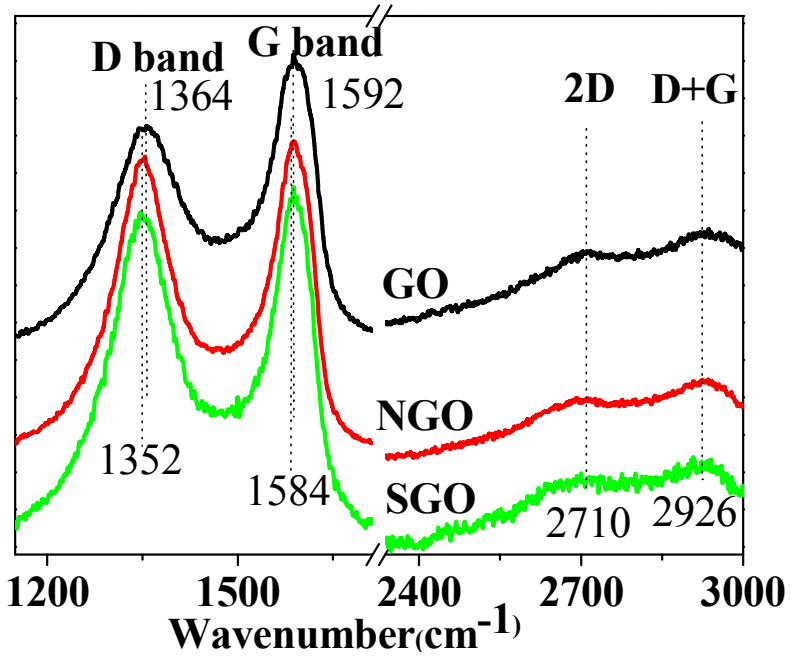

Fig. 6 Raman spectra of GO, NGO and SGO

The increase in the electrical conductivity of the graphene materials often signifies the efficiency of a particular reduction method, therefore the structure difference of SGO and NGO may explain the difference in the electrical conductivity. The electrical conductivity was measured using a four-probe method and was calculated using the formula: $\sigma = 1/\rho$, where ρ (unit: $\Omega \cdot cm$) referred to the electrical resistivity that can be obtained by the test directly. After GO reduction by basic divalent sulfide, SGO reached a relatively higher electrical conductivity of 7690 S/m, however, NGO showed some lower conductivity at 6578.9 S/m, probably due to the presence of some saturated carbon C-H moiety and the smaller average size of aromatic domains. In other words, GO can undergo more effective deoxygenation and the larger-area π-conjugated structure in presence of basic divalent sulfide.

3.2 Graphene oxidation modification mechanism

The mechanism for the chemical modification of GO remained obscure, but it had been explained by SN_2 nucleophilic reactions[8, 12]. The basal-plane of GO is highly populated with 1, 2-epoxides and hydroxyl groups while the edge-plane mainly consists of carboxyl and carbonyl groups. Those oxygen containing groups account for the structural defects that lead graphene oxide to deviate from the state of pristine graphene. Pablo A. Denis and C. Pereyra Huelmo[28] gave us a better understand of S incorporation mechanism under high temperature condition, however, inspired by the reduction of anthraquinone and the role of sulfur in the transformations of sedimentary organic matter,[34] a possible mechanism of GO modification by basic divalent sulfide species at low temperature (<100 ^{o}C) was provided. Basic divalent sulfide species is often utilized in synthetic chemistry for electrophilic addition and nucleophilic substitution reactions. On one hand, acting as the reducing agent basic divalent sulfide played a role on removing the oxygen containing groups. On the other hand, basic divalent sulfide species are nucleophilic in nature and react with GO via SN_1 or SN_2 pathway. The proposed process was listed in Scheme 1, through which the conjugated structure was restored. Although the reductive reaction induced by basic divalent sulfide species was expected to have little influence on the elimination of marginal oxygen-containing groups owing to the high-energy barrier[16], Basic divalent sulfide species were thought to be doped in GO (process was listed in Scheme 2). Sulfide might act as the medium to connect the adjacent GO sheets, therefore large area graphene sheets formed. At the same time, a part of the structural defects were repaired by the basic divalent sulfide modification, thus enhancing the electrical conductivity. The dope mechanism was speculated in Scheme 3.

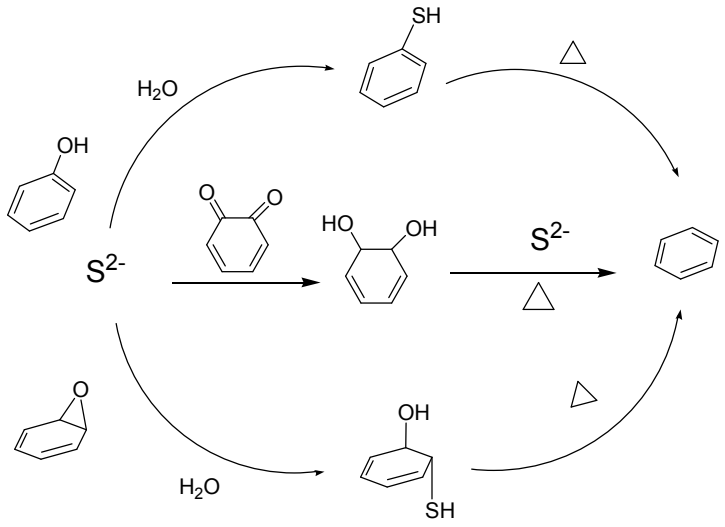

Scheme 1: Possible deoxygenation mechanism by the basic divalent sulfide

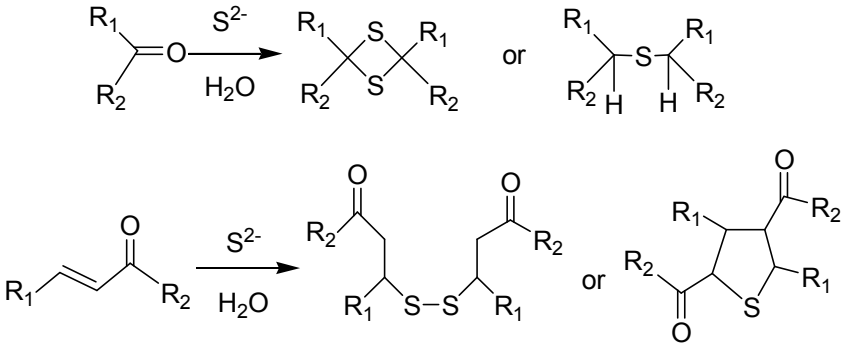

Scheme 2: The basic divalent sulfide incorporation process

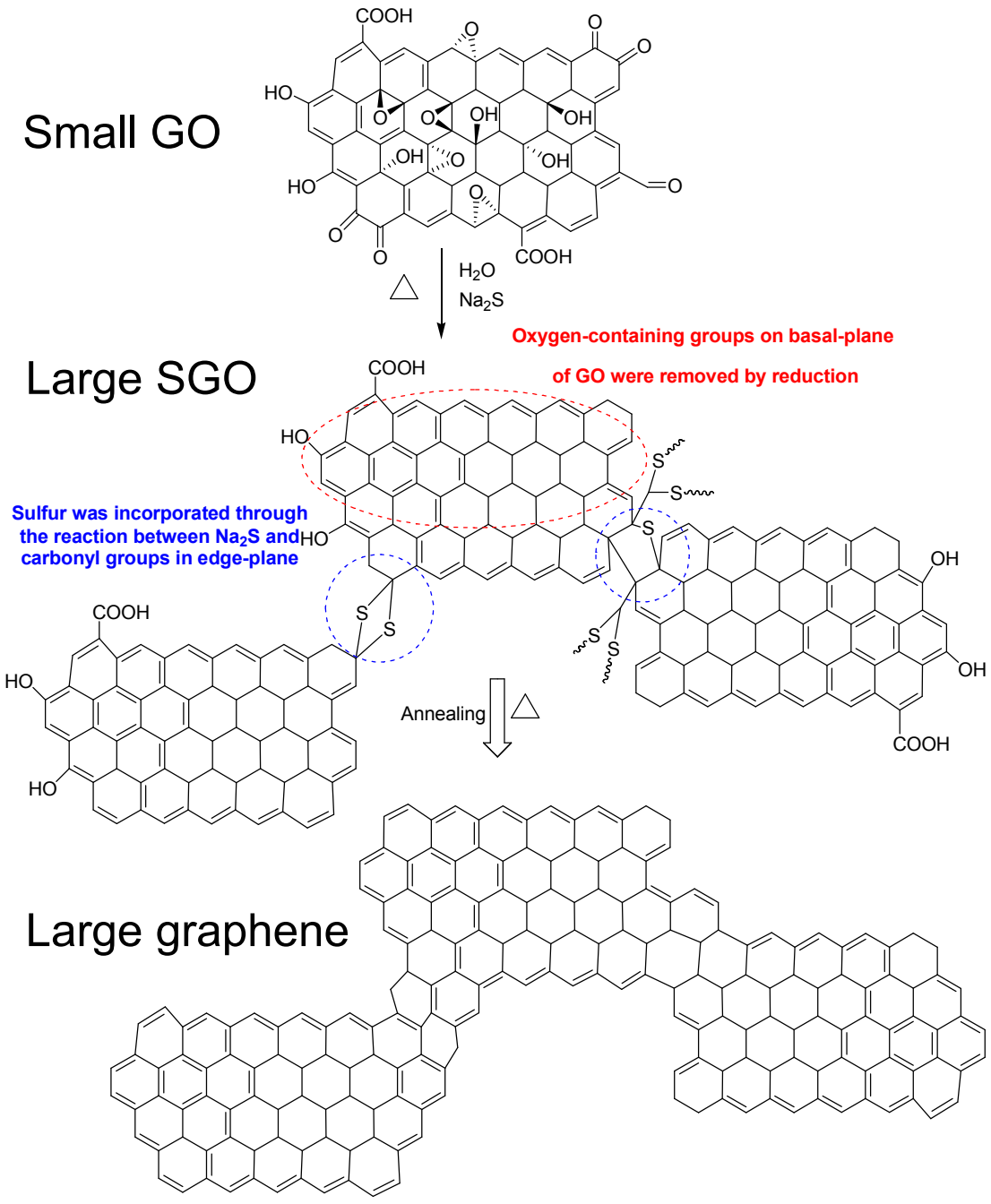

Scheme 3: The larger area graphene formation process from the small GO sheet

3.3 Biomass conversion into HMF over SGO without annealing

Recently the selective conversion of fructose and glucose (or cellulose) into HMF has attracted significant interest because HMF and its derivatives are potential substitutes for petroleum-based chemicals. The conversion of glucose into HMF is generally achieved by two

steps: glucose is first isomerized to fructose using catalysts based on a Lewis acid or a base, followed by fructose dehydration to yield HMF under acidic conditions.[35] $CrCl_2$ exhibited excellent performance for the isomerization of glucose into fructose and further dehydration of the generated fructose in an ionic liquid solvent, and HMF yield was in the range of 60–70%.[36] However, the homogeneous chromium based catalysts have serious environmental and operational problems for the large-scale production of HMF from glucose.

Table 1 HMF yields from carbohydrates over different catalyst

Catalysts	Surface area (m^2 g^{-1})	HMF yield /Selectivity (mol%)			
		Fructose (140 °C/4h)	Glucose (140 °C/4h)	Cellobiose (140 °C/4h)	Cellulose (180 °C/2h)
SGO	360	73.4	76.9	77.8	66.2
NGO	465	45.4	49.8	36.7	30.2
GO	867	84.6	56.9	51.1	49.4
TRGO	760	68.93	1.56	2.10	8.29

Conditions: 0.9g carbohydrate, 0.03g catalyst, 5mL 1-ethyl-3-methylimidazolium sodium bromide ([EMIM] Br) and 4h.

It is well know that the introduction of heteroatoms could increases reactivity of graphene, and this effect was attributed to the strong charge redistribution induced by the dopants[28]. Herein, the S incorporation in graphene might act as reactive sites to promote the transform from glucose to fructose. SGO, NGO and GO were used to catalyze fructose,

glucose, cellobiose and cellulose conversion to HMF (Table 1). GO display a better performance in fructose dehydration to HMF, and HMF yield over GO achieved 84.6%. However, glucose, cellobiose and cellulose were difficult to be conversed into HMF over GO. When SGO was used as catalysts in [EMIM]Br, 73.4% HMF yield was obtained from fructose dehydration, but SGO also showed an excellent performance in HMF synthesis from glucose, cellobiose and cellulose. However, HMF yields from fructose, glucose, cellobiose and cellulose over NGO declined to 45.4%, 49.8%, 36.7% and 30.2%. The plausible mechanisms of glucose conversion to HMF over SGO were proposed (Scheme 4). Namely, glucose was isomerized into fructose over Lewis basic sulfide sites of SGO, while the marginal COOH, phenolic hydroxyl group and a trace of SO_3H played a key role in fructose dehydration into HMF. Although TRGO have high surface area, it displayed no activity for glucose conversion into HMF.

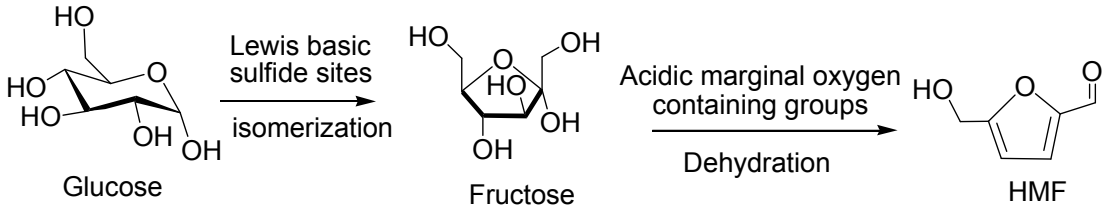

Scheme 4: HMF formation process over SGO

4. Conclusion

The basic divalent sulfide is an excellent reducing agents for GO deoxygenation, and it can be incorporated into GO. When GO was modified by basic divalent sulfide species, the formation of saturated C-H was restrained and π-conjugated structure was more easily restored. There existed some C-S bonds in SGO, and the existence of the basic divalent sulfide species acted as the medium to connect adjacent GO sheets to form the large-area conjugated

sp^2-carbon network, which made SGO to have a relatively higher electrical conductivity of 7690 S/m. However, NGO showed some lower conductivity at 6578.9 S/m, due to some saturated C-H moiety, C-N specie and the smaller average size of aromatic domains in NGO. When SGO was used as catalysts to catalyze biomass conversion in [EMIM]Br, 73.4% HMF yield was obtained from fructose dehydration, and SGO showed an excellent performance in HMF formation from glucose, cellobiose and cellulose. Those results further indicated that the basic divalent sulfide was incorporated into SGO and the residual oxygen-containing groups were the acidic marginal oxygen-containing groups. At the same time, a possible mechanism of GO modification by basic divalent sulfide species was provided, that is the basic divalent sulfide species, acting as the reducing agent, are capable of removing the abundant hydroxyl and epoxide functionalities on basal-plane of GO to obtain the conjugated structure, while basic divalent sulfide species can be incorporated to connect adjacent GO sheets.

Acknowledgements

The authors are grateful for the financial support of the National and Tianjin Natural Science Foundation of China (nos. 21376177 and 12JCZDJC29800 and 15JCZDJC7000). This work is also supported by China National Textile and Apparel Council (J201406) and Science and technology innovation project of Shanxi Province (2014101002).

References

1 M. Ishigami, J.H. Chen, W.G. Cullen, M.S. Fuhrer, E.D. Williams, Nano Lett. 2007, 7,1643.

2 S. Stankovich, D.A. Dikin, G.H.B. Dommett, K.M. Kohlhaas, E.J. Zimney, E.A. Stach, R.D. Piner, S.T. Nguyen, R.S. Ruoff, Nature , 2006, 442, 282.

3 H.C. Schniepp, J. L. Li, M.J. McAllister, H. Sai, M. Herrera-Alonso, D.H. Adamson, R.K. Prud'homme, R. Car, D.A. Saville, I.A. Aksay, J. Phys. Chem. B 2006, 110, 8535.

4 C. Berger, Z. M. Song, T. B. Li, X.B. Li, A. Y. Ogbazghi, R. Feng, Z.T. Dai, A.N. Marchenkov, E.H. Conrad, P.N. First, W.A. De Heer, J. Phys. Chem. B 2004, 108, 19912.

5 K. S. Kim, Y. Zhao, H. Jang, S.Y. Lee, J.M. Kim, K.S. Kim, J.H. Ahn, P. Kim, J.Y. Choi, B.H. Hong, Nature, 2009, 457, 706.

6 S. Stankovich, D.A. Dikin, R.D. Piner, K.A. Kohlhaas, A. Kleinhammes, Y.Y. Jia, Y. Wu, S.T. Nguyen, R.S. Ruoff, Carbon 2007, 45, 1558.

7 W. Chen, L. Yan, P.R. Bangal, Carbon 2010, 48, 1146.

8 X.F. Gao, J. Jang, S. Nagase, J. Phys. Chem. C 2009, 114, 832.

9 H.J. Shin, K.K. Kim, A. Benayad, S.M. Yoon, H.K. Park, I.S. Jung, M.H. Jin, H.K. Jeong, J.M. Kim, J.Y. Choi, Y.H. Lee, Adv. Funct. Mater. 2009, 19, 1987.

10 M.J. Fernandez-Merino, L. Guardia, J.I. Paredes, S. Villar-Rodil, P. Solis-Fernandez, A. Martinez-Alonso, J.M.D. Tascon, J. Phys. Chem. C 2010, 114, 6426.

11 P.F. Song, J.P. Zhao, J.H. Du, W.C. Ren, H.M. Cheng, Carbon. 2010, 48, 4466.

12 W.F. Chen, L.F. Yan, P.R. Bangal, J. Phys. Chem. C 2010, **114**, 19885.

13 T.N. Zhou, F. Chen, K. Liu, H. Deng, Q. Zhang, J.W. Feng, Q. Fu, Nanotechnology. 2011, **22**, 045704.

14 H.Y. Fu, X.L. Qu, W. Chen, D.Q. Zhu, Environ. Toxicol. Chem. 2014, **33**, 2647.

15 W. Gao, L.B. Alemany, L.J. Ci, P. M. Ajayan, Nature Chem. 2009, **1**, 403.

16 Y. Su, X. Gao, J. Zhao, Carbon 2014, **67**, 146.

17 Y. Long, C. Zhang, X. Wang, J. Gao, W. Wang, Y. Liu, J. Phys. Chem. 2011, **21**, 13934.

18 A. Lerf, H. He, M. Forster, J. Klinowski, J. Phys. Chem. B 1998, **102**, 4477.

19 J.F. Tijero, M. Oliet, J.C. Burillo, F. Rodriguez, Ind. Eng. Chem. Res. 1991, **30**, 1791.

20 S.J. Park, J. An, R.D. Piner, I. Jung, D.X. Yang, A. Velamakanni, S.T. Nguyen, R.S. Ruoff, Chem. Mater. 2008, **20**, 6592-6594.

21 Y.X. Xu, H. Bai, G. Lu, C. Li, G.Q. Shi, J. Am. Chem. Soc. 2008, **130**, 5856.

22 O.C. Compton, S.T. Nguyen, Graphene Oxide, Small. 2010, **6**, 711.

23 D.C. Luo, G. X. Zhang, J. F. Liu, X.M. Sun, J. Phys. Chem. C 2011, **115**, 11327.

24 D. Li, M.B. Mueller, S. Gilje, R.B. Kaner, G.G. Wallace, Nat. Nanotechnol. 2008, 3, 101.

25 D. Briggs, G. Beamson, High Resolution XPS of Organic Polymers: Thescienta ESCA300 Database. John Wiley and Sons: New York, 1992.

26 R.J. Waltman, J. Pacansky, C.W. Bates Jr, Chem Mater. 1993, **5**, 1799.

27 S. Zhang, Y.Y. Shao, H.G. Liao, M.H. Engelhard, G. Yin, Y.H. Lin, ACS Nano 2011, **5**, 1785.

28. P.A. Denis, C. Pereyra Huelmo, Carbon 2015, **87**, 106.

29 D.S. Knight, W.B. White, J. Mater. Res. 1989, **4**, 385.

30 S. Park, J.H. An, R.D. Piner, I. Jung, D.X. Yang, A. Velamakanni, S.T. Nguyen, R.S. Ruoff, Chem Mater. 2008, **20**, 6592.

31 F. Tuinstra, J. L. Koenig, J. Chem. Phys. 1970, 53, 1126.

32 M. A. Pimenta, G. Dresselhaus, M.S. Dresselhaus, L.G. Cancado, A. Jorio, R. Saito, Phys Chem Chem Phys. 2007, 9, 1276.

33 M.S. Dresselhaus, A. Jorio, M. Hofmann, G. Dresselhaus, R. Saito, Nano Lett 2010, **10**, 751.

34 Z. Aizenshtat, E.B. Krein, M. A. Vairavamurthy, T.P. Goldstein, Role of Sulfur in the Transformations of Sedimentary Organic Matter: A Mechanistic Overview. ACS Symposium Series, Geochemical Transformations of Sedimentary Sulfur, Chapter 2, 612(1995)16-37.

35 M.E. Zakrzewska, E. Bogel-Łukasik, R. Bogel-Łukasik, Chem. Rev. 2011, **111**, 397–417.

36 H. Zhao, J.E. Holladay, H. Brown, Z.C. Zhang, Science 2007, **316**, 1597.